Biochimica et Biophysica Acta 1837 (2014) 1990–1997

Contents lists available at ScienceDirect

Biochimica et Biophysica Acta

journal homepage: www.elsevier.com/locate/bbabio

The hierarchy of transition metal homeostasis: Iron controls manganese accumulation in a unicellular cyanobacterium

Shir Sharon [a,1], Eitan Salomon [a,1], Chana Kranzler [a], Hagar Lis [a], Robert Lehmann [b], Jens Georg [c], Hagit Zer [a], Wolfgang R. Hess [c], Nir Keren [a,*]

[a] Department of Plant and Environmental Sciences, The Alexander Silberman Institute of Life Sciences, Edmond J. Safra Campus, Givat Ram, The Hebrew University of Jerusalem, Jerusalem, Israel
[b] Institute for Theoretical Biology, Humboldt University Berlin, Invalidenstraße 43, D-10115 Berlin, Germany
[c] Genetics and Experimental Bioinformatics Group, Faculty of Biology, University of Freiburg, Freiburg, Germany

ARTICLE INFO

Article history:
Received 8 June 2014
Received in revised form 17 September 2014
Accepted 18 September 2014
Available online 28 September 2014

Keywords:
Iron
Manganese
Homeostasis
Transcription
Photosynthesis
Synechocystis 6803

ABSTRACT

Iron and manganese are part of a small group of transition metals required for photosynthetic electron transport. Here, we present evidence for a functional link between iron and manganese homeostasis. In the unicellular cyanobacterium, *Synechocystis* sp. PCC 6803, Fe and Mn deprivation resulted in distinct modifications of the physiological status. The effect on growth and photosynthetic activity under Fe limitation were more severe than those observed under Mn limitation. Moreover, the intracellular elemental quotas of Fe and Mn were found to be linked. Fe limitation reduced the intracellular Mn quota. Mn limitation did not exert a reciprocal effect on Fe quotas. Microarray analysis comparing Mn and Fe limitation revealed a stark difference in the extent of the transcriptional response to the two limiting conditions, reflective of the physiological responses. The effects of Fe limitation on the transcriptional network are widespread while the effects on Mn limitation are highly specific. Our analysis also revealed an overlap in the transcriptional response of specific Fe and Mn transporters. This overlap provides a framework for explaining Fe limitation induced changes in Mn quotas.

1. Introduction

Transition metals play an important role as cofactors in a multitude of cellular process including growth, development and metabolism [1–3]. In photosynthetic organisms, iron (Fe) is an essential cofactor in the photosynthetic apparatus, raising its required intracellular quota substantially above that of non-photosynthetic organisms [4–8]. Poor Fe bioavailability limits primary productivity in both aquatic and terrestrial ecosystems where it is often present at subnanomolar concentrations and bound by a heterogeneous pool of organic ligands [9–11].

Among photosynthetic organisms, cyanobacteria have especially high Fe requirements in part due to a high photosystem I (PSI, 12 Fe atoms) to photosystem II (PSII, 3 Fe atoms) ratio [12–15]. Studies on iron limitation in cyanobacteria uncovered a complex cascade of responses which involve transcriptional regulators [16–21], non-coding RNA [8], iron storage proteins [5,22] and a number of transporters including the Fe^{2+} transporter, FeoAB and the Fe^{3+} transporter, FutABC [23–26]. Iron limitation induces a remodeling of the photosynthetic apparatus where IsiA becomes the major chlorophyll binding protein and IsiB replaces ferredoxin as an electron carrier [27–31].

In addition to iron, manganese (Mn) is indispensable in the photosynthetic apparatus. Located within a pocket formed by PSII proteins on the lumenal side of the thylakoid membrane, Mn is a central component of the catalytic Mn_4CaO_5 cluster in the oxygen-evolving complex on the donor side of PSII [13,32]. Accordingly, one of the most common phenotypes of Mn limitation is a reduction in oxygen evolution capacity [33,34].

Current knowledge on manganese transport and homeostasis in cyanobacteria is more limited. In *Synechocystis* sp. strain PCC 6803 (henceforth *Synechocystis* 6803), MntCAB was identified as a high affinity Mn transporter [35]. The transcription of the *mntCAB* operon is induced under Mn limitation and controlled by the ManS/R two-component system [36,37]. However, Mn transport assays suggested the existence of one or several additional low affinity transport systems [38]. A periplasmic Mn binding protein, MncA, was also identified but its connection to Mn transport is still unknown [39].

In both freshwater and marine water bodies, Mn is present at nanomolar levels [9,40–47], predominantly in its soluble Mn^{2+} form. In a few studies Mn was shown to be a limiting factor for diatoms, although mostly in co-limitation scenarios together with iron [9,48,49]. In cyanobacteria, changes in Mn concentration within the environmentally relevant range affected the oligomerization state and function of PSI and PSII in *Synechocystis* 6803 [34].

In many natural environments, essential minerals and nutrients are scarce and their supply irregular [40,50,51]. Organisms have to regulate

* Corresponding author. Tel.: +972 2 6585233; fax: +972 2 6584425.
E-mail address: nir.ke@mail.huji.ac.il (N. Keren).
[1] Equal contribution.

http://dx.doi.org/10.1016/j.bbabio.2014.09.007
0005-2728/

mineral transport, storage and usage to make the most of the available resources. This is complicated further by overlapping intracellular pathways [52]; a situation that can be advantageous, for example, when Fe containing protein cytochrome c_6 can replace the copper protein plastocyanin [53]; or co-limiting such as when urea utilization is dependent on nickel as a cofactor in ureases [54].

While the effects of Fe and Mn limitation in cyanobacteria were documented individually, environmental variability and the intricacy of biological systems raises questions regarding the physiological and regulatory relationships between these two transition metals in a photosynthetic organism. Indeed, Fe limited cells contain less intracellular Mn, eluding to a possible interaction between the homeostasis of these two metals [19].

In this study we compared the effects of manganese and iron bioavailability on the model cyanobacterium *Synechocystis* 6803. We monitored physiological status, elemental composition and the transcriptional response during the transition into Fe and Mn limitation. Our findings provide insight into the cross-talk between Fe and Mn homeostasis.

2. Materials and methods

2.1. Trace metal clean techniques

All glassware was soaked overnight in 3.7% HCl and then washed with double distilled water. All stock solutions were prepared using double distilled water and analytical grade chemicals. Preparations for mass spectrometry analysis were conducted in a trace metal clean facility [22].

2.2. Growth conditions

Synechocystis 6803 was grown in modified BG11 medium containing 16 μM EDTA (YBG11; [22]) in glass Erlenmeyer flasks. Cultures were maintained under constant shaking, illuminated with 60 μmol photons m^{-2} s^{-1} at 30 °C. Prior to an experiment, cultures were spun down and washed twice in a 20 mM of 2-(N-morpholino) ethanesulfonic acid (MES) and 10 mM ethylenediaminetetraacetic acid (EDTA; Kd, 10^{24}) pH 5.0 buffer, in order to remove excess metal ions. Cultures where resuspended in one of four media types:

1) **Control** media; 10 μM Fe and 1 μM Mn.
2) **0Mn**; Mn was omitted from the media. Residual Mn concentrations in the medium were in the 0–2 nM range, as confirmed by ICP-MS analysis.
3) **0Fe**; Fe was omitted from the media and 50 μM of the siderophore, deferoxamine B (DFB; $K_{Fe(III)L} = 10^{31}$, [55]) was added in addition to the EDTA. Residual Fe concentrations in the medium were in the sub μM range, as confirmed by ICP-MS analysis. In the presence of excess DFB practically all of the residual iron was complexed. While Fe(III):DFB complexes are bioavailable to *Synechocystis* 6803 through the reduction of the complex prior to transport of Fe(II), the rate of transport is quite low and not sufficient to support growth [56]. The addition of excess DFB further decreases Fe bioavailability in the medium by competing with the cells for any free Fe ions in the media [19].
4) **0Fe0Mn**; contained DFB and no added Mn or Fe.

Starting cultures were all grown in full YBG11 media containing 10 μM Fe and 1 μM Mn buffered by 16 μM EDTA. Experiments were started with mid-log phase cells (10^7 to 10^8 cells ml^{-1}) that were treated as described in the section above and diluted to 0.03 $OD_{730\ nm}$ (2.5×10^5 cells ml^{-1}). A viability test was conducted at day 7 of the limitation experiments. Cells were harvested and adjusted to the same $OD_{730\ nm}$. Samples were spotted on BG11 plates. The resulting spots were scanned after three days and their intensity determined with ImageJ software. Chemical speciation of transition metals in the media was calculated using Visual MINTEQ, 3.0 (http://www2.lwr.kth.se/English/Oursoftware/vminteq/).

2.3. Spectroscopy

Cell growth was monitored with optical density measurements at 730 nm using a Cary 3000 spectrophotometer (Varian, CA, USA). $OD_{730\ nm}$ was calibrated to cell number using a hemocytometer. The difference between the calculated calibration curve for Control and Fe or Mn limited cells was smaller than 10%. In order to obtain the intracellular metal ion quota, 10 mL were removed from each culture and the intracellular quota was determined as described in Shcolnick et al. [19]. The procedure was applied to all samples, including time 0 samples. Metal ion concentrations were determined using an inductively coupled plasma mass spectrometer (ICP-MS; PerkinElmer-Elan, MA, USA).

In order to measure metal content in the cellular envelope layer [57], 20 mL were removed from the cultures on day 7. ICP-MS measurements were conducted on 10 mL as is (total) and on three fractions: Spent medium, EDTA wash (periplasmic fraction) and Intracellular [57]. The Spent medium fraction was obtained after centrifugation at 9000 *g*. The Wash fraction was obtained after suspension and centrifugation of the pellet in the MES:EDTA wash buffer (see Section 2.2) for twenty minutes. The pellet contained the intracellular fraction.

PSII photochemical yield $[(F_m - F_0) / F_m = F_v/F_m]$ was measured with an Imaging PAM (Heinz Walz GmbH, Effeltrich, Germany). F_0 was determined with illumination by the modulated measuring light (Excitation wavelength = 450 nm, Emission wavelength > 665 nm). F_m was measured with an actinic light intensity of 286 μmol photons m^{-2} s^{-1} in the presence of 10 μM DCMU. PSI activity was measured as P700 photo-oxidation using the Joliot-type spectrophotometer [58]. In order to block electron flow to PSI, 10 μM DCMU and 10 μM 2,5-dibromo-3-methyl-6-isopropylbenzoquinone (DBMIB) were added.

2.4. Oxygen evolution

Oxygen evolution rates were measured in the same triplicate samples used for F_v/F_m measurements. Oxygen concentrations were monitored with a Clark type electrode. Illumination was set at a saturating intensity of 2000 μmol photons m^{-2} s^{-1}.

2.5. RNA isolation and analysis

Cultures used for microarray analysis were collected after 48 hours, centrifuged at 9000 *g* at 4 °C, resuspended in phenol–chloroform extraction (Tri-reagent, Sigma-Aldrich, USA) and frozen. A microarray was used, covering all genes and intergenic regions for which transcripts were detected before [59,60]. RNA was labeled directly for microarray hybridization. The arrays were hybridized in quadruplicates with pooled RNA from the different limitation conditions to detect transcripts which were upregulated or downregulated under specific conditions. The microarray data are available in the GEO database. A complete description of array design was provided by Georg et al., 2009.

Raw expression data were subjected to a background correction by subtraction using the R package *limma*. Probes with smaller mean expression over all samples than the negative control spots were discarded. This reduced the total number of probes by 7869 (Out of 20293). The raw arrays were normalized using cyclic LOESS (locally weighted scatterplot smoothing) using the *normalizeBetweenArrays* function of *limma*. Due to strong deviations in one of the three repeats for the 0Mn and 0Fe0Mn conditions, the corresponding replicates were excluded from further analysis. The remaining normalized probe values are probe-wise summarized using *lmFit* (package limma) before averaging all probes setwise to yield gene expression values.

The annotation of genes to functional categories was obtained from Cyanobase, which distinguishes 18 main and 75 subfunctions. The main

categories of antisense and NC-RNA were added to this set to reflect the additional information on the microarrays.

The supplemental spreadsheet (Supplemental file 2) includes the calculated fold change values for all of the coding and non-coding transcripts. The threshold for significant differential expression was set to 1.5 fold for the high confidence set (genes which exhibit an absolute |fold change| > 1.5 under at least one condition) and 1 for the low confidence set. Supplemental file 3 provides a graphical representation of fold change values for each probe. Samples were collected from the experiment presented in Figs. 1A & 3.

Quantitative RT-PCR was conducted for *rnpB*, an established housekeeping gene in *Synechocystis* 6803 [61] and for the *futA2* and *mntC* transcripts. 10 ng of cDNA were used for each sample. Q-RT-PCR was carried out with the Absolute Blue qPCR SYBR Green ROX mix (Thermo Scientific) with a Rotor Gene 6000 qPCR machine (Qiagen, Valencia, CA). Primer sequences were: *futA2*: FP: ATTCTTCACGGCATTACAAC RP: TGGATACGCTCAATCAGTTC; *mntC*: FP: GGGAAACAGAGGAGAAAAAG RP: TGGATTCCACCACTAACTTG; rnpB: FP: GGAGTTGCGGATTCCTGTCA RP: CGTTACCCAGCAAGTTTGGC. Primer efficiency was confirmed by genomic PCR as well as by a melting curve from each primer Tm up to 95 °C. Two independent cultures were measured with a least two technical repeats. Standard curves were used for relative quantification. Each data set was internally normalized to *rnpB* and the resulting relative transcript accumulation values were compared to the Control.

2.6. Immunoblot analysis

Synechocystis 6803 cells were grown in control, 0Fe 0Mn and 0Fe0Mn conditions. After 7 days the cultures were collected. The ensuing protein extraction was conducted as described previously [34]. Samples equivalent to 1 μg chlorophyll were loaded on 14% SDS-PAGE gels. The blots were incubated with primary antibodies against PsaA, PsbA and IsiA (Agrisera, Vännäs, Sweden).

3. Results and discussion

3.1. Growth response to Fe and Mn limitation

Synechocystis 6803 cultures were grown under 0Fe, 0Mn and combined 0Fe0Mn conditions (Fig. 1). The residual bioavailable Fe concentration in 0Fe was lower than the residual Mn concentration in 0Mn. However, this chemical asymmetry is reflective of many natural conditions in which the concentration of bioavailable Fe is in the sub-nM range and the concentration of bioavailable Mn is in the low nM range (Martin et al. 1990). Under these limiting conditions growth was impaired as compared to sufficient control conditions. Under 0Fe, cell growth stopped completely by day four of the experiment (0Fe, Fig. 1). Cultures grown without Mn exhibited slower growth rates as compared to the control culture but still performed better than 0Fe (0Mn, Fig. 1). The combined 0Fe0Mn conditions were similar to 0Fe with no additional effect on growth (0Fe0Mn, Fig. 1). The viability of the cultures was tested qualitatively using a spotting assay on BG11 plates. All cultures were viable, however, small differences were observed between the viability of iron limited and iron sufficient cultures (Supplemental file 1, Fig. S1).

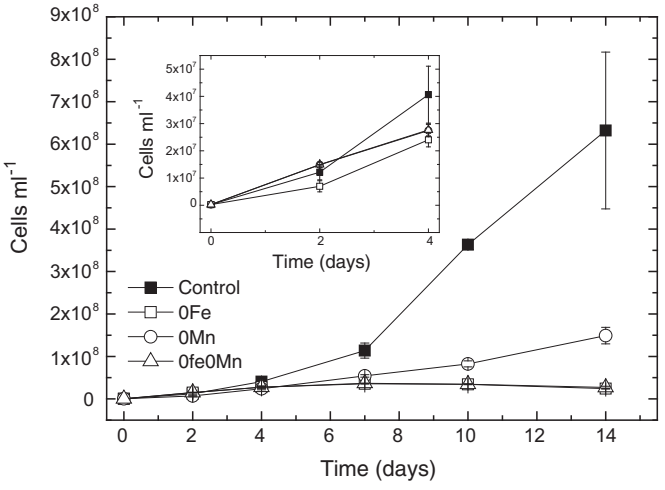

Fig. 1. Effects of Mn and Fe availability on biomass accumulation rates. *Synechocystis* 6803 cultures were grown under 0Fe, 0Mn, 0Fe0Mn and control conditions. Biomass was monitored as optical density at 730 nm. Cellular content was determined using a calibration curve (Salomon et al. 2013). Insert, close up view of the first 4 days of the experiment. Error bars represent standard deviation with n = 3.

3.2. Elemental quota dynamics in limited cultures

In order to probe for possible relationships between Fe and Mn homeostasis the elemental composition within the cells was monitored during the progression of Mn and Fe limitation. ICP-MS (inductively coupled plasma mass spectrometry) provided data on the intracellular quota of a range of transition metals (Fig. 2 and Supplemental file 1,

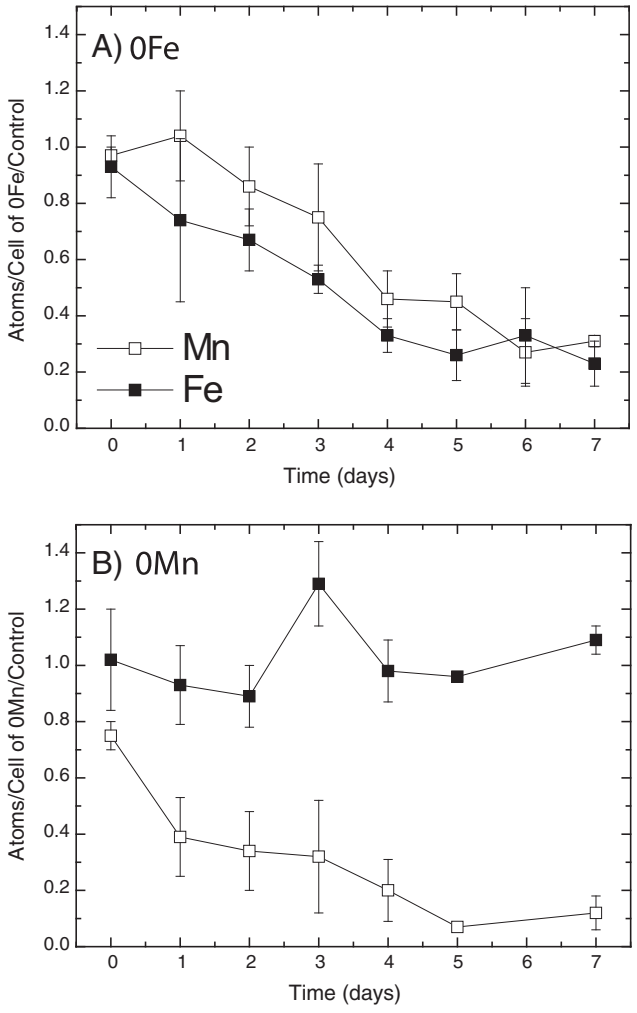

Fig. 2. Intracellular iron and manganese quotas. *Synechocystis* 6803 cultures were analyzed for their internal metal quotas during one week of growth in non-limited (control) and 0Fe (A) or 0Mn (B) conditions. The intracellular Fe and Mn content, normalized to control cells, is presented. The data represents the mean value of four independent experiments with three duplicate cultures each. Due to different sampling regimes between the four experiments SD values are calculated from 3–4 repeats for each point. Data for additional metals is presented in Supplemental file 1, Figs. S2–S3.

Fig. S2). For most of these, no distinct trend was observed (Supplemental file 1, Fig. S2). In contrast, Mn did not accumulate in 0Fe cells (Fig. 2A). Intracellular Mn quotas dropped in parallel with the drop in Fe quotas (Fig. 2A) despite abundant levels of extracellular Mn. This finding is consistent with the lower Mn quota observed in Fe-limited *Synechocystis* 6803 before [19]. Statistical analysis of four experimental repeats yielded a correlation coefficient of 0.94 ± 0.08 between Mn and Fe, in the 0Fe treatments (Supplemental file 1, Fig. S2, Table S1). This correlation was much larger than for any of the other metals analyzed (Supplemental file 1, Fig. S2, Table S1). Fe content, on the other hand, did not decrease in response to Mn limitation (Fig. 2B). Specific and significant correlations with Mn quotas were not detected for any of the other metal species (Supplemental file 1 Fig. S3, Table S2).

As the stability constant of Mn(III):DFB is quite high ($10^{29.9}$), the addition of excess DFB can drive the oxidation of Mn(II) despite the low stability constant of DFB for Mn(II) ($10^{8.8}$, [62]). In addition, Mn(III) disproportionates to Mn(II) and Mn(VI) [63]. These chemical reactions can potentially impose Mn limitation in the presence of DFB. In order to confirm that DFB is not inducing Mn limitation in our experimental setup we calculated the Mn speciation in 0Fe medium prior to the addition of DFB. The presence of EDTA effectively buffers Mn(II), maintaining 98.3% of the dissolved Mn as Mn(II)EDTA. The higher stability of the Mn(II):EDTA ($10^{13.6}$, Martell and Smith 1982) complex as compared to the Mn(II):DFB complex will slow down the oxidation processes of Mn(II) by DFB considerably.

Furthermore, the presence of cyanobacterial cells in the media also plays a role. Cyanobacterial cells quickly remove Mn the media [57]. A large excess of Mn(II) is stored in the envelope layer of the cells and can only be removed by mM concentrations of EDTA. This extracellular Mn pool is then slowly transported into the cell to supply the internal need. Using the wash protocol developed in Keren et al. 2002 we measured the size of the envelope layer pool in cells grown for 7 days in the different media. Control cells contained 4.7×10^6 atoms/cell in this pool, 0Fe cells 4.6×10^6 atoms/cells and 0Mn cells 3.9×10^5 atoms/cell. Values in the range of 10^6 atoms/cell are equivalent to the intracellular Mn quota of replete cells. With this much extra Mn we can be confident that the chemical speciation of Mn in the presence of DFB does not impose a significant Mn limitation in 0Fe media and that the root cause of the dependence of the intracellular Mn quota on the Fe quota is dependent on the biology of the system.

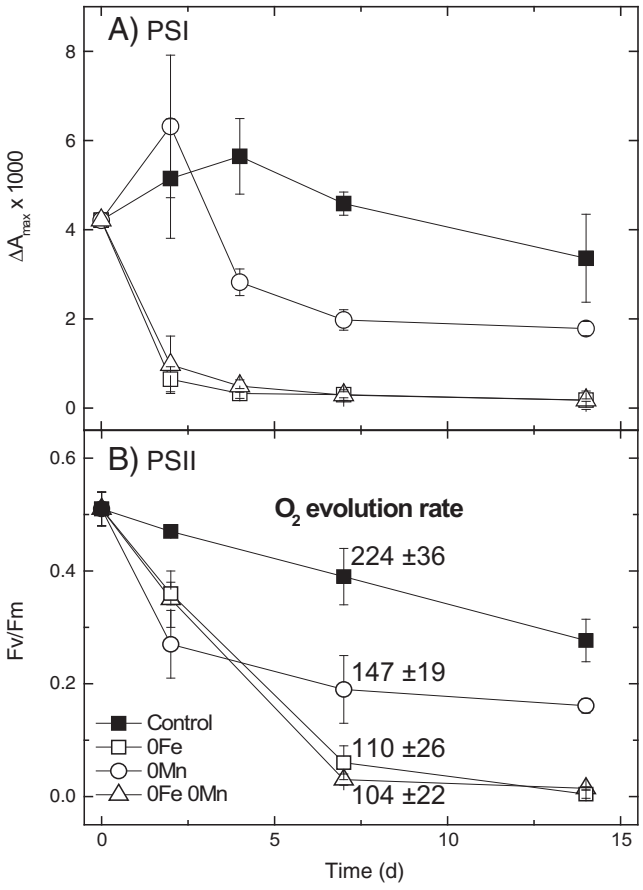

Fig. 3. Photosynthetic activity. The activity of PSI and PSII during transition into metal limitation was determined. (A) PSI activity was measured as the maximal change in P700 absorbance ΔA_{max} (Salomon and Keren 2011). (B) PSII activity was measured as the maximal chlorophyll fluorescence yield F_v/F_m. Standard error values were derived from three biological replicates. Whole chain O_2 evolution rates were measured on day 7 and are presented next to the corresponding F_v/F_m value in the graph (in units of μmol O_2 mg^{-1} chl h^{-1}, n = 3).

3.3. Physiological effects of Fe and Mn limitation on the photosynthetic apparatus

Fe and Mn both serve as indispensable co-factors in photosynthesis. We compared the effects of Fe and Mn limitation on the function of the photosynthetic apparatus (Fig. 3). PSI function significantly decreased within two days of transfer into either 0Fe or 0FeMn, consistent with the measured reduction of iron quotas observed after transfer into 0Fe (Fig. 2). A decrease in PSI function was expected in response to 0Fe as PSI is one of the most abundant iron containing protein complexes in the cell. However, PSI activity was also impaired in 0Mn (Fig. 3A). 0Mn effects on PSI function were slower to develop and were of a lesser extent than under 0Fe (Fig. 3A). This loss of PSI activity cannot be associated with Fe quotas that remained high in 0Mn (Fig. 2B). These results are in line with a recent study demonstrating changes in PSI activity and organization under Mn limitation [34]. This drop in PSI activity was suggested to accommodate the loss of PSII activity in the limited cells.

A loss of PSII photochemical efficiency, measured as F_v/F_m, was observed in the 0Fe and 0Fe0Mn treatments (Fig. 3B). A similar effect on F_v/F_m was reported for *Synechocystis* 6803 and *Synechococcus* sp. PCC 7942, using different measurement techniques [64,65]. F_v/F_m in the 0Mn treatment dropped to about half of its initial value within two days and retained the same level throughout the experiment (Fig. 3B). Oxygen evolution measurements were conducted in parallel to confirm that the decrease in photosynthetic activity depicted by F_v/F_m was not biased by IsiA fluorescence [64,66,67]. On day 7, oxygen evolution rates in 0Mn cultures decreased to 65% of the control while the rates in the 0Fe and 0Fe0Mn cultures dropped to 50% of the control values (Fig. 3B).

3.4. Transcriptional response to Mn and Fe limitation

To probe the regulatory events that lead to the differential response to Mn and Fe limitation, transcriptional profiles of control and limited cultures were studied by microarray analysis (Tables 1–2). RNA was extracted two days after transfer into the limiting medium. At that time we could observe the initiation of the physiological response to the limiting conditions but growth rates were unchanged. Therefore, the transcriptional responses unique to Fe and Mn limitation were expected to be more prominent while the general stress response to be minimal.

3.5. Global transcriptional trends

The most apparent result is the difference in the overall extent of the transcriptional response to Mn and Fe limitation (Table 1). Iron limitation (0Fe) effects were stronger than those of 0Mn in all of the functional categories. The transcriptional network controlling the response to Fe limitation is large and includes regulation on the levels of transcription and degradation of relevant mRNAs [20,68,69]. In our dataset, the most

Table 1
Gene expression patterns in response to metal limitation.
Global effects of metal limitation on gene expression in entire functional classes. For each set of genes with the same functional annotation (rows), the number of genes with positive (+) or negative fold changes (−) between control and the various conditions (columns) were counted. The minimum absolute fold change was set to 0.5 to capture the global trend rather than significance in differential expression. The average fold change observed for the corresponding functional class is provided numerically (Group avg.) and visualized by the corresponding cell color. The histogram at the bottom provides the distribution of the transcriptional changes.

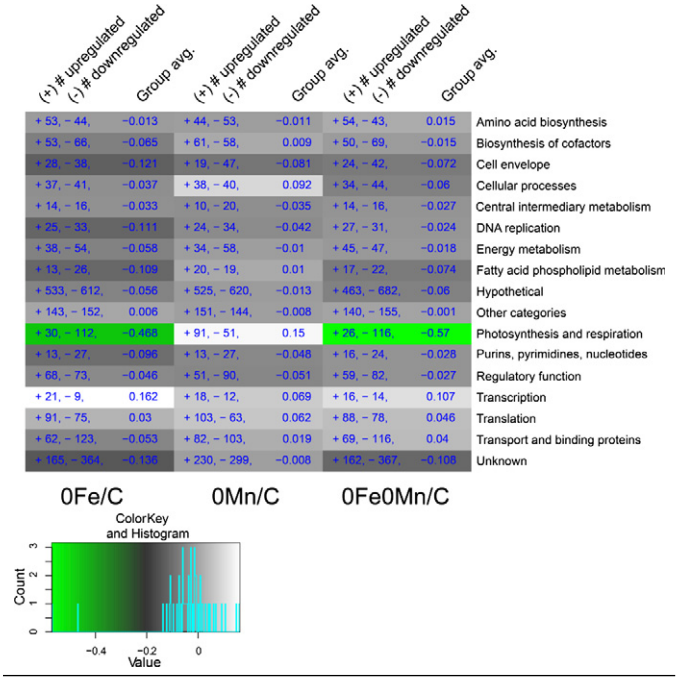

Table 2
Transcript levels of metal transporters.
Transcription profile under 0Fe, 0Mn or 0Fe0Mn conditions. The analysis includes the Mg, Cu, Zn, Mn and Fe transporters. Fold changes are visualized by the corresponding cell color. The effect on the transcription levels of *futA2* and *mntC* were verified by Q-RT-PCR. The transcripts were internally normalized to *rnpB*. Fold change in transcript levels for *futA2* were 0Fe/C 10.1 ± 0.4, 0Mn/C 0.09 ± 0.03, 0Fe0Mn/C 8.7 ± 0.6 and for *mntC* 0Fe/C 0.2 ± 0.01, 0Mn/C 4.5 ± 0.25, 0Fe0Mn/C 0.58 ± 0.09 (n = 2). Both expression patterns are comparable to the microarray results.

Transported ion	Gene name	Gene symbol	Condition		
			0Fe/C	0Mn/C	0Fe0Mn/C
Fe	feoA	slr1392	1.55	0.23	1.43
	feoB	ssr2333	2.34	0.28	2.28
	futC	sll1878	1.75	0.50	1.55
	futA1	slr1295	3.44	1.85	3.50
	futA2	slr0513	2.53	0.85	2.16
	futB	slr0327	0.07	0.04	0.13
	OM porin	sll1206	4.14	0.18	3.87
	OM porin	sll1406	1.27	0.13	1.15
Mn	mntC	sll1598	0.47	2.38	1.94
	mntA	sll1599	0.19	2.10	1.29
	mntB	sll1600	−0.16	1.84	0.91
Zn	znuB	slr2044	−0.04	0.06	−0.01
	znuC	slr2045	−0.52	−0.18	−0.39
	znuB	slr2043	−0.25	0.07	−0.01
Cu	ctaA	slr1950	0.05	0.04	0.08
	pacS	sll1920	−0.33	−0.24	−0.22
Mg	mgtE	slr1216	−0.20	−0.09	−0.12
	mgtC	slr0014	−0.10	−0.11	−0.11

striking difference is in the photosynthesis and respiration category. These transcripts where strongly repressed under 0Fe and 0Fe0Mn. A functional enrichment analysis was performed for a high confidence set of transcripts (|fold change| > 1.5), which were separated into groups of co-expressed genes. Enriched functions are almost exclusively photosynthesis and respiration-related (Supplemental file 2, Functional enrichment tab). Interestingly, in contrast to 0Fe conditions, transcription of the photosynthesis and respiratory category genes was induced under 0Mn (Table 1).

On the protein level, western blot analysis revealed a decrease in the abundance of the PSII core protein PsbA under 0Fe and 0Fe0Mn (Fig. 4A), but not under control conditions. This decrease coincides with the physiological effects of Fe limitation (Fig. 3B). In contrast, under 0Mn, PsbA levels were similar to those of the control (Fig. 4A). A similar correlation was observed for the PSI subunit, PsaA. PsaA concentrations significantly decreased under 0Fe and 0Fe0Mn (Fig. 4B). Under 0Mn, PsaA levels remained higher than under 0Fe but, as in the iron limited samples, low MW fragments were observed indicating that the protein is being actively degraded (see [34], as well).

The transcriptional response to 0Fe and 0Mn or 0Mn and 0Fe0Mn treatments exhibited no significant correlation (0.32 and 0.26, respectively; Supplemental file 1, Fig. S4). A strong correlation was observed between 0Fe and 0Fe0Mn (Pearson correlation coefficient of 0.89, Supplemental file 1, Fig. S4). This is consistent with the physiological data – both 0Fe and 0Fe0Mn treatments exhibited similar phenotypes suggesting that the iron limitation dominates the response. Taken together, these data suggest that Fe limitation and Mn limitation induce a distinct regulatory cascade on the photosynthetic apparatus.

3.6. Effects on specific non-coding RNAs

The microarrays used in this study also probed a group of non-coding RNAs [59]. The effects of 0Fe where thoroughly studied and the results found here are in line with previous studies [8,20,69]. In the case of 0Mn this is the first report on the role of non-coding RNAs. We found a total of 25 asRNAs and 24 NC-RNAs whose levels changed under 0Mn in the high confidence set (Supplemental file 2, NC-RNA tab). This represents a significant enrichment in the response of non-coding RNAs among the set of differentially expressed mRNAs (hypergeometrical test, $p < 0.004$, using high confidence set data). In contrast, asRNAs were not over-represented (hypergeometrical test $p < 0.96$).

A small number of NC-RNAs responded specifically to 0Mn (Fig. 5). Among them is NC-106 whose transcript was enhanced under 0Mn. Its location shortly upstream of the start codon of *psbD2* and downstream of the mapped strong start site of transcription [60] indicates that NC-106 represents the 5′UTR rather than an independent NC transcript. However, the *psbD2* transcript is depressed under 0Fe and 0Fe0Mn and increased only together with NC-106 under 0Mn (Supplemental file 2, NC-RNA tab). Therefore, a regulatory mechanism acting on the *psbD2* 5′UTR appears likely.

Out of seven exclusively 0Mn-repressed probes, five are in NC-RNAs (Supplemental file 2, NC-RNA tab). NC-392, NC-1410/NC-1413 probes overlap by 7 bp and NC-1481/NC-1171 probes overlap almost completely. Interestingly, two of the three Mn-stress repressed NC-RNAs (NC-1413/NC-1410 and NC-392) have a NADH-dehydrogenase subunit as the closest neighbor. The distance of 121 bp between NC-1413/NC-1410 and *ndhF3* coincides with the recently mapped start site of transcription that is located 241 nt upstream of the *ndhF3 [69]* start codon [69]. NC-392 is located only 52 bp away from the start of the NADH dehydrogenase subunit 3 gene (*ndhC*, *slr1279*). However, there are two distinct start sites of transcription for *ndhC*, pointing at the possible existence of an

independently accumulating 5′UTR, further supported by the fact that 0Mn represses both, *slr1279* and NC-392, but at different degrees (−0.73 and −2.23 fold, respectively).

3.7. Effects on specific genes

The extent of transcriptional changes for individual genes under all experimental conditions is presented in Supplemental file 1 Table S3. The transcripts are divided into groups which responded only to the 0Fe (A), 0Mn (B) or 0Fe0Mn (C) as well as groups which responded to combinations of these conditions (D–G).

A small group of noteworthy transcripts was strongly up or down regulated under all conditions (Supplemental file 1, Table S3G). The *sbtB* gene (*slr1513*) is part of an operon coding for the high affinity Na^+/HCO_3^- transporter SbtA [70]. Both genes presented a similar transcriptional profile (Supplemental file 1, Table S3D). Among the transcripts that were upregulated under all limiting conditions we found *slr1667* (Supplemental file 1, Table S3G). This gene was identified as a putative target gene for the DNA binding cAMP receptor SYCRP1 [71]. This regulatory network is thought to be involved in controlling motility. Because the twitching motility of *Synechocystis* 6803 requires extensive remodeling of protein complexes located at the cell surface, a coordination between this apparatus and the induction of uptake systems for certain metal ions might involve SyCRP1.

The most down-regulated genes code for *flv* related proteins [72]. *sll0219* codes for a flavoprotein (Flv2) that was found to be induced by both high light and carbon limitation [73]. *sll0218* codes for an unknown protein in the *flv4-sll0218-flv2* operon. Flv4 transcripts exhibited a similar trend, but to a smaller extent (Supplemental file 2, LCS genes tab). The function of the proteins coded by this operon was suggested to be photoprotection of PSII [20,74].

Many of the 0Fe affected genes were involved in alleviating iron limitation stress by modulating photosynthetic activity. Consistent with the western blot analysis (Fig. 4C), we saw an increase in the iron stress inducible transcripts, *isiA* and *isiB*, in 0Fe and 0Fe0Mn conditions. Iron transporter genes were also induced under 0Fe and 0Fe0Mn conditions. Iron transport in Fe limited *Synechocystis* 6803 is strongly dependent on reduction of Fe(III) species to Fe(II) [26,56]. In iron limited cultures, Fe reduction and Fe transport rates are 100 times higher than in Fe-replete cultures. Accordingly, under 0Fe, transcription of *feoB*, an Fe(II) transporter, was induced 2.34 fold of the control (Table 2). A gene encoding for a putative Fe transporter in the outer membrane was strongly upregulated as well (*sll1206*, Table 2). Transcription of the genes encoding for Fe(III) binding proteins, *futA1* and *futA2* [25,75], were also induced in response to Fe limitation (Table 2). Located in the periplasm [76], FutA2 is part of the Fe(III) ABC transporter, FutABC. FutA2 plays a role in periplasmic metal partitioning and seems to be involved in the homeostasis of several metals in addition to iron [76,77]. The location of FutA1 is not fully determined. It was detected in both soluble and membrane fractions [78]. A knockout strain for *futA1* displayed enhanced *futA2* transcription and iron uptake rates suggesting a regulatory relationship between these proteins [26].

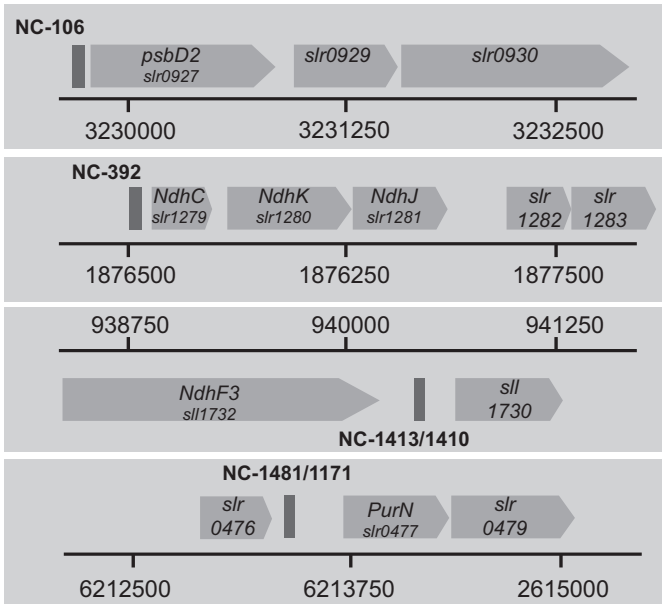

Fig. 5. NC-RNAs. The genomic position of NC-RNAs and of neighboring genes, discussed in Section 3.6, is provided on the corresponding scale bar. Genes are presented as arrows and NC-RNAs as boxes.

Under 0Mn and 0Fe0Mn the strongest up-regulation was observed in genes coding for the MntCAB transporter and for PSII subunits. The induction of these genes was significant under both conditions but stronger under 0Mn (Table 2 and Supplemental file 1 Table S3B). Interestingly, several iron transport related genes were also induced under 0Mn conditions. This effect was restricted to iron related transport genes as other metal transporters were all slightly down regulated in 0Mn (Table 2). Specifically, transcription of both *futA1* (*slr1295*) and *futA2* (*slr0513*) was up-regulated by Mn limitation.

It is possible that these proteins may play a role in Mn acquisition as well. Mn(II) and Fe(III) complexes have very similar geometries. Both have similar electronic configurations, high spin (d^5) states, and can adopt octahedral or tetrahedral coordination spheres [80]. Therefore, it is reasonable to assume that the biological system, transporters and sensors alike, would find it difficult to tell the two apart. Such

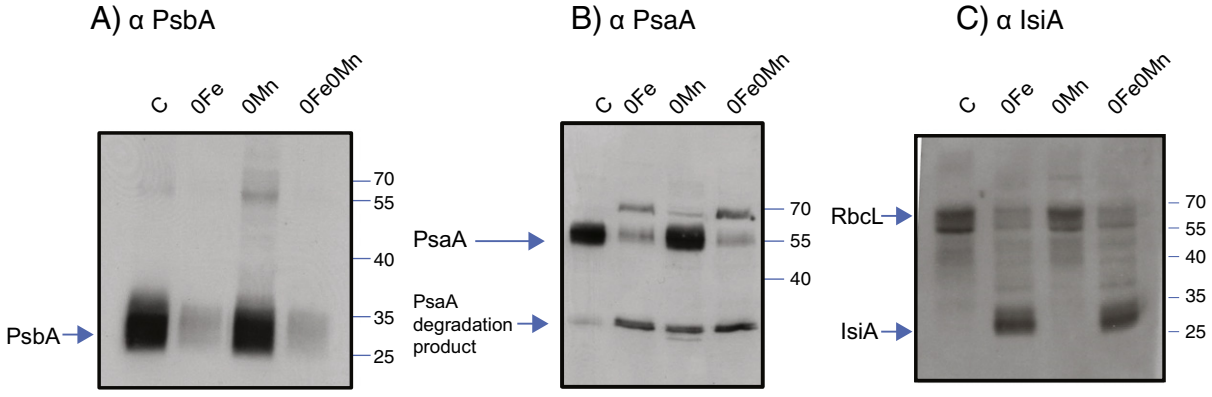

Fig. 4. Western blot analysis. Control (C), 0Fe, 0Mn and 0Fe0Mn cells were harvested at day 7. Protein samples were loaded on an equal chlorophyll content basis. Immunoblot assays were carried against PSII and PSI core proteins (PsbA (A) and PsaA (B), respectively) and against the iron stress inducible protein IsiA (C). The αIsiA antibody cross-reacts with the large subunit of Rubisco — RbcL (according to the manufacturer's data). The locations of the proteins and degradation fragments are marked.

"promiscuity" of metal binding proteins has been demonstrated for Mn/Cu/Zn, Cu/Co and Fe/Mn specificities [39,78,79]. The IRT1 transporter from Arabidopsis was shown to transport Mn/Fe/Zn [81].

Transcription of the Fe(III) permease, *futB*, remained effectively unchanged in both Fe and Mn limitation suggesting that FutA2 abundance and metal binding in the periplasm may determine transport capability. A similar role in regulating the periplasmic iron pool was suggested for FutA2 in reductive iron transport [26]. In contrast, ferrous ions adopt a different configuration than either Fe(III) or Mn(II) (low spin or high spin d^6, octahedral coordination only). Therefore, Fe(II) uptake cannot support efficient Mn(II) transport as efficiently as Fe(III) transport. Indeed, under 0Mn, *feoB* transcript abundance remained similar to that of the control. This suggested low affinity transport mode may account for the unidentified low affinity transport system detected by Bartsevich and coworkers [38].

When iron is limiting, the Fe transport system shifts towards high-efficiency Fe(II) intake [26], thus limiting Mn(II) uptake rates via the Fe(III) transport route. This may explain the noted decrease in Mn levels under Fe insufficiency. Accordingly, it raises the possibility that iron limited cells may be starved for Mn as well. Surprisingly, the transcription of the *mntCAB* operon was only slightly induced in 0Fe conditions as compared to Zn, Cu or Mg transporters (Table 2). This indicates that the cells are not "sensing" severe Mn limitation under these conditions despite the dramatic decrease in intracellular Mn quotas (Table 2). The system in charge of Mn sensing are the ManS/R two component regulators that react to Mn concentrations in the periplasmic space, where Mn is abundant [36,37]. The genes coding for this system showed no transcriptional dependence on the conditions tested (Supplemental file 1, Table S3).

4. Conclusions

In this study we observed limited transcriptional responses under 0Mn, as compared to 0Fe and 0Fe0Mn treatments. In fact, the specific Mn limitation regulon seems to be composed mostly of the *mntCAB* operon with only a few NC-RNAs reacting in a 0Mn-specific fashion. However, PSII activity decreased, albeit to a smaller extent than under 0Fe (Figs. 3 & 4). The smaller influence of 0Mn on the physiology and the transcriptional profile, taken together with the dominance of iron limitation under 0Fe0Mn conditions, suggest that the repercussions of Mn limitation in natural environments are minor as compared to Fe.

The issue can be stated in terms of the possible "dangers" of photosynthetic electron transport. Mn limitation would reduce the rate of water splitting thus lowering the occupancy of electron carriers. This is a relatively safe condition, even though it imposes slower growth rates [34]. In fact, depressing PSII activity was demonstrated to improve the acclimation to nitrogen limiting conditions [58] and to protect against PSI photodamage [82]. Fe limitation affects electron acceptors primarily and would promote the over-reduction of electron carriers, a much more dangerous situation that requires swift, dedicated cellular responses. Accordingly, the transcriptional and physiological response to Fe limitation is swift and extensive. The coordinated decrease in Mn quotas, under these conditions, can serve as part of this response mechanism, possibly by reducing the rate of electron flow through Mn containing PSII.

Acknowledgments

We would like to thank Adi Salomon, Uri Raviv and Avi Bino for their assistance.

This work was supported by the Federal Ministry of Education and Research (BMBF) grant 0316165 awarded to WRH; The Einstein Foundation Berlin and the Israeli Science Foundation grant (806/11) awarded to NK.

Appendix A. Supplementary data

Supplementary data to this article can be found online at http://dx.doi.org/10.1016/j.bbabio.2014.09.007.

References

[1] K. Hantke, Iron and metal regulation in bacteria, Curr. Opin. Microbiol. 4 (2001) 172–177.
[2] E.L. Walker, E.L. Connolly, Time to pump iron: iron-deficiency-signaling mechanisms of higher plants, Curr. Opin. Plant Biol. 11 (2008) 530–535.
[3] R. Hansch, R.R. Mendel, Physiological functions of mineral micronutrients (Cu, Zn, Mn, Fe, Ni, Mo, B, Cl), Curr. Opin. Plant Biol. 12 (2009) 259–266.
[4] J.R. Raven, M.C.W. Evans, R.E. Korb, The role of trace metals in photosynthetic electron transport in O_2 evolving organisms, Photosynth. Res. 60 (1999) 111–149.
[5] N. Keren, R. Aurora, H.B. Pakrasi, Critical roles of bacterioferritins in iron storage and proliferation of cyanobacteria, Plant Physiol. 135 (2004) 1666–1673.
[6] J.A. Raven, Iron acquisition and allocation in stramenopile algae, J. Exp. Bot. 64 (2013) 2119–2127.
[7] S. Shcolnick, N. Keren, Metal homeostasis in cyanobacteria and chloroplasts. Balancing benefits and risks to the photosynthetic apparatus, Plant Physiol. 141 (2006) 805–810.
[8] U. Duhring, I.M. Axmann, W.R. Hess, A. Wilde, An internal antisense RNA regulates expression of the photosynthesis gene *isiA*, PNAS 103 (2006) 7054–7058.
[9] J.H. Martin, R.M. Gordon, S.E. Fitzwater, Iron in Antarctic waters, Nature 345 (1990) 156–158.
[10] P.G. Falkowski, R.T. Barber, V. Smetacek, Biogeochemical controls and feedbacks on ocean primary production, Science 281 (1998) 200–206.
[11] M.L. Guerinot, Improving rice yields — ironing out the details, Nat. Biotechnol. 19 (2001) 417–418.
[12] M. Rogner, P.J. Nixon, B.A. Diner, Purification and characterization of photosystem I and photosystem II core complexes from wild-type and phycocyanin-deficient strains of the cyanobacterium *Synechocystis* PCC 6803, J. Biol. Chem. 265 (1990) 6189–6196.
[13] Y. Umena, K. Kawakami, J.R. Shen, N. Kamiya, Crystal structure of oxygen-evolving photosystem II at a resolution of 1.9 Å, Nature 473 (2011) 55–65.
[14] M. Muramatsu, Y. Hihara, Acclimation to high-light conditions in cyanobacteria: from gene expression to physiological responses, J. Plant Res. 125 (2012) 11–39.
[15] Y. Mazor, D. Nataf, H. Toporik, N. Nelson, Crystal structures of virus-like photosystem I complexes from the mesophilic cyanobacterium *Synechocystis* PCC 6803, e-life 3 (2014) e01496.
[16] H.C. Riethman, L.A. Sherman, Purification and characterization of an iron stress-induced chlorophyll protein from the cyanobacterium *Anacystis nidulans* R2, Biochim. Biophys. Acta 935 (1988) 141–151.
[17] A.K. Singh, L.M. McIntyre, L.A. Sherman, Microarray analysis of the genome-wide response to iron deficiency and iron reconstitution in the cyanobacterium *Synechocystis* sp. PCC 6803, Plant Physiol. 132 (2003) 1825–1839.
[18] L. Houot, M. Floutier, B. Marteyn, M. Michaut, A. Picciocchi, P. Legrain, J.C. Aude, C. Cassier-Chauvat, F. Chauvat, Cadmium triggers an integrated reprogramming of the metabolism of *Synechocystis* PCC 6803, under the control of the *slr1738* regulator, BMC Genomics 8 (2007) 350.
[19] S. Shcolnick, T.C. Summerfield, L. Reytman, L.A. Sherman, N. Keren, The mechanism of iron homeostasis in the unicellular cyanobacterium *Synechocystis* sp. PCC 6803 and its relationship to oxidative stress, Plant Physiol. 150 (2009) 2045–2056.
[20] M.A. Hernandez-Prieto, V. Schon, J. Georg, L. Barriera, J. Varela, W.R. Hess, M.E. Futschik, Iron deprivation in *Synechocystis*: inference of pathways, non-coding RNAs, and regulatory elements from comprehensive expression profiling, G3-Genes Genomes Genet. 2 (2012) 1475–1495.
[21] A. Gonzalez, V.E. Angarica, J. Sancho, M.F. Fillat, The FurA regulon in *Anabaena* sp. PCC 7120: in silico prediction and experimental validation of novel target genes, Nucleic Acids Res. 42 (2014) 4833–4846.
[22] S. Shcolnick, Y. Shaked, N. Keren, A role for MrgA, a DPS family protein, in the internal transport of Fe in the cyanobacterium *Synechocystis* sp. PCC 6803, Biochim. Biophys. Acta 1767 (2007) 814–819.
[23] H. Katoh, A.R. Grossman, N. Hagino, T. Ogawa, A gene of *Synechocystis* sp. strain PCC 6803 encoding a novel iron transporter, J. Bacteriol. 182 (2000) 6523–6524.
[24] H. Katoh, N. Hagino, A.R. Grossman, T. Ogawa, Genes essential to iron transport in the cyanobacterium *Synechocystis* sp. strain PCC 6803, J. Bacteriol. 183 (2001) 2779–2784.
[25] H. Katoh, N. Hagino, T. Ogawa, Iron-binding activity of FutA1 subunit of an ABC-type iron transporter in the cyanobacterium *Synechocystis* sp. strain PCC 6803, Plant Cell Physiol. 42 (2001) 823–827.
[26] C. Kranzler, H. Lis, O.M. Finkel, G. Schmetterer, Y. Shaked, N. Keren, Coordinated transporter activity shapes high-affinity iron acquisition in cyanobacteria, ISME J. 8 (2014) 409–417.
[27] D.E. Laudenbach, M.E. Reith, N.A. Straus, Isolation, sequence-analysis, and transcriptional studies of the flavodoxin gene from *Anacystis nidulans* R2, J. Bacteriol. 170 (1988) 258–265.
[28] D.E. Laudenbach, N.A. Straus, Characterization of a cyanobacterial iron stress-induced gene similar to *psbC*, J. Bacteriol. 170 (1988) 5018–5026.
[29] R.L. Burnap, T. Troyan, L.A. Sherman, The highly abundant chlorophyll-protein complex of iron deficient *Synechococcus* sp. PCC 7942 (CP43) is encoded by the *isiA* gene, Plant Physiol. 103 (1993) 893–902.
[30] C. Kutzki, B. Masepohl, H. Bohme, The *isiB* gene encoding flavodoxin is not essential for photoautotrophic iron limited growth of the cyanobacterium *Synechocystis* sp. strain PCC 6803, FEMS Microbiol. Lett. 160 (1998) 231–235.

[31] T.S. Bibby, J. Nield, J. Barber, Iron deficiency induces the formation of an antenna ring around trimeric photosystem I in cyanobacteria, Nature 412 (2001) 743–745.
[32] M.M. Najafpour, A.N. Moghaddam, S.I. Allakhverdiev, Govindjee, Biological water oxidation: lessons from nature, Biochim. Biophys. Acta 1817 (2012) 1110–1121.
[33] G. MCheniae, I.F. Martin, Photoreactivation of manganese catalyst in photosynthetic oxygen evolution, Plant Physiol. 44 (1969) 351–360.
[34] E. Salomon, N. Keren, Manganese limitation induces changes in the activity and in the organization of photosynthetic complexes in the cyanobacterium *Synechocystis* sp. strain PCC 6803, Plant Physiol. 155 (2011) 571–579.
[35] V.V. Bartsevich, H.B. Pakrasi, Molecular identification of an ABC transporter complex for manganese — analysis of a cyanobacterial mutant strain impaired in the photosynthetic oxygen evolution process, EMBO J. 14 (1995) 1845–1853.
[36] T. Ogawa, D.H. Bao, H. Katoh, M. Shibata, H.B. Pakrasi, M. Bhattacharyya-Pakrasi, A two-component signal transduction pathway regulates manganese homeostasis in *Synechocystis* 6803, a photosynthetic organism, J. Biol. Chem. 277 (2002) 28981–28986.
[37] K. Yamaguchi, L. Suzuki, H. Yamamoto, A. Lyukevich, I. Bodrova, D.A. Los, I. Piven, V. Zinchenko, M. Kanehisa, N. Murata, A two-component Mn^{2+} sensing system negatively regulates expression of the *mntCAB* operon in *Synechocystis*, Plant Cell 14 (2002) 2901–2913.
[38] V.V. Bartsevich, H.B. Pakrasi, Manganese transport in the cyanobacterium *Synechocystis* sp. PCC 6803, J. Biol. Chem. 271 (1996) 26057–26061.
[39] S. Tottey, K.J. Waldron, S.J. Firbank, B. Reale, C. Bessant, K. Sato, T.R. Cheek, J. Gray, M.J. Banfield, C. Dennison, N.J. Robinson, Protein folding location can regulate manganese binding versus copper- or zinc-binding, Nature 455 (2008) 1138–1142.
[40] R. Chester, J.H. Stoner, The distribution of particulate organic carbon and nitrogen in some surface waters of the world ocean, Mar. Chem. 2 (1974) 263–275.
[41] M.L. Bender, G.P. Klinkhammer, D.W. Spencer, Manganese in seawater and the marine manganese balance, Deep-Sea Res. 24 (1977) 799–812.
[42] G.P. Klinkhammer, M.L. Bender, The distribution of manganese in the Pacific Ocean, Earth Planet. Sci. Lett. 46 (1980) 361–384.
[43] W.M. Landing, K.W. Bruland, The contrasting biogeochemistry of iron and manganese in the Pacific Ocean, Geochim. Cosmochim. Acta 51 (1987) 29–43.
[44] W.G. Sunda, S.A. Huntsman, Effect of sunlight on redox cycles of manganese in the southwestern Sargasso sea, Deep-Sea Res. A 35 (1988) 1297–1317.
[45] Z. Chase, K.S. Johnson, V.A. Elrod, J.N. Plant, S.E. Fitzwater, L. Pickell, C.M. Sakamoto, Manganese and iron distributions off central California influenced by upwelling and shelf width, Mar. Chem. 95 (2005) 235–254.
[46] S. Yemenicioglu, S. Erdogan, S. Tugrul, Distribution of dissolved forms of iron and manganese in the Black Sea, Deep-Sea Res. II 53 (2006) 1842–1855.
[47] R. Middag, H.J.W. de Baar, P. Laan, P.H. Cai, J.C. van Ooijen, Dissolved manganese in the Atlantic sector of the Southern Ocean, Deep-Sea Res. II 58 (2011) 2661–2677.
[48] L.E. Brand, W.G. Sunda, R.R.L. Guillard, Limitation of marine phytoplankton reproductive rates by zinc, manganese, and iron, Limnol. Oceanogr. 28 (1983) 1182–1198.
[49] G. Peers, N.M. Price, A role for managanese in superoxide dismutases and growth of iron-deficient diatoms, Limnol. Oceanogr. 49 (2004) 1774–1783.
[50] F.M.M. Morel, N.M. Price, The biogeochemical cycles of trace metals in the oceans, Science 300 (2003) 944–947.
[51] F.M.M. Morel, The co-evolution of phytoplankton and trace element cycles in the oceans, Geobiology 6 (2008) 318–324.
[52] M.A. Saito, T.J. Goepfert, J.T. Ritt, Some thoughts on the concept of colimitation: three definitions and the importance of bioavailability, Limnol. Oceanogr. 53 (2008) 276–290.
[53] G. Sandmann, P. Boger, Copper induced exchange of plastocyanin and cytochrome C533 in cultures of *Anabaena variabilis* and *Plectonema boryanum*, Plant Sci. Lett. 17 (1980) 417–424.
[54] P.R. Hawtin, H.T. Delves, D.G. Newell, The demonstration of nickel in the urease of *Helicobacter pylori* by atomic-absorption spectroscopy, FEMS Microbiol. Lett. 77 (1991) 51–54.
[55] T. Kiss, E. Farkas, Metal binding ability of Desferrioxamine B, J. Incl. Phenom. Mol. Recognit. Chem. 32 (1998) 385–403.
[56] C. Kranzler, H. Lis, Y. Shaked, N. Keren, The role of reduction in iron uptake processes in a unicellular, planktonic cyanobacterium, Environ. Microbiol. 13 (2011) 2990–2999.
[57] N. Keren, M.J. Kidd, J.E. Penner-Hahn, H.B. Pakrasi, A light-dependent mechanism for massive accumulation of manganese in the photosynthetic bacterium *Synechocystis* sp. PCC 6803, Biochemistry 41 (2002) 15085–15092.
[58] E. Salomon, L. Bar-Eyal, S. Sharon, N. Keren, Balancing photosynthetic electron flow is critical for cyanobacterial acclimation to nitrogen limitation, Biochim. Biophys. Acta 1827 (2013) 340–347.
[59] J. Georg, B. Voss, I. Scholz, J. Mitschke, A. Wilde, W.R. Hess, Evidence for a major role of antisense RNAs in cyanobacterial gene regulation, Mol. Syst. Biol. 5 (2009) 305.
[60] J. Mitschke, J. Georg, I. Scholz, C.M. Sharma, D. Dienst, J. Bantscheff, B. Voss, C. Steglich, A. Wilde, J. Vogel, W.R. Hess, An experimentally anchored map of transcriptional start sites in the model cyanobacterium *Synechocystis* sp. PCC 6803, PNAS 108 (2011) 2124–2129.
[61] F. Pinto, C.C. Pacheco, D. Ferreira, P. Moradas-Ferreira, P. Tamagnini, Selection of suitable reference genes for RT-qPCR snalyses in cyanobacteria, PLoS One 7 (2012) e34983.
[62] W. Duckworth, G. Sposito, Siderophore-manganese(III) interactions. I. Air oxidation of manganese(II) promoted by desferrioxamine B, Environ. Sci. Technol. 39 (2005) 6037–6044.
[63] R.E. Trouwborst, B.G. Clement, B.M. Tebo, B.T. Glazer, G.W. Luther, Soluble Mn(III) in suboxic zones, Science 313 (2006) (1955–1957).
[64] S. Sandstrom, A.G. Ivanov, Y.I. Park, G. Oquist, P. Gustafsson, Iron stress responses in the cyanobacterium *Synechococcus* sp. PCC 7942, Physiol. Plant. 116 (2002) 255–263.
[65] T.J. Ryan-Keogh, A.I. Macey, A.M. Cockshutt, et al., The cyanobacteria chlorophyll binding protein IsiA acts to increase the in vivo effective absorption cross section of PSI under iron limitation, J. Phycol. 48 (2012) 145–154.
[66] A.K. Singh, L.A. Sherman, Reflections on the function of IsiA, a cyanobacterial stress-inducible, Chl-binding protein, Photosynth. Res. 93 (2007) 17–25.
[67] J.M. Fraser, S.E. Tulk, J.A. Jeans, D.A. Campbell, T.S. Bibby, A.M. Cockshutt, Photophysiological and photosynthetic complex changes during iron starvation in *Synechocystis* sp. PCC 6803 and *Synechococcus elongatus* PCC 7942, PLoS One 8 (2013) e59861.
[68] C. Kranzler, M. Rudolf, N. Keren, E. Schleiff, Iron in Cyanobacteria, Genomics Cyanobact. 65 (2013) 57–105.
[69] M. Kopf, S. Klähn, I. Scholz, J.K.F. Matthiessen, W.R. Hess, B. Voss, Comparative analysis of the primary transcriptome of *Synechocystis* sp. PCC 6803, DNA Res. (2014), http://dx.doi.org/10.1093/dnares/dsu018 (in press).
[70] M. Shibata, H. Katoh, M. Sonoda, H. Ohkawa, M. Shimoyama, H. Fukuzawa, A. Kaplan, T. Ogawa, Genes essential to sodium-dependent bicarbonate transport in cyanobacteria — function and phylogenetic analysis, J. Biol. Chem. 277 (2002) 18658–18664.
[71] H. Yoshimura, S. Yanagisawa, M. Kanehisa, M. Ohmori, Screening for the target gene of cyanobacterial cAMP receptor protein SYCRP1, Mol. Microbiol. 43 (2002) 843–853.
[72] Y. Helman, D. Tchernov, L. Reinhold, M. Shibata, T. Ogawa, R. Schwarz, I. Ohad, A. Kaplan, Genes encoding a-type flavoproteins are essential for photoreduction of O_2 in cyanobacteria, Curr. Biol. 13 (2003) 230–235.
[73] P.P. Zhang, Y. Allahverdiyeva, M. Eisenhut, E.M. Aro, Flavodiiron proteins in oxygenic photosynthetic organisms: photoprotection of photosystem II by Flv2 and Flv4 in *Synechocystis* sp. PCC 6803, PLoS One 4 (2009) e5331.
[74] P.P. Zhang, M. Eisenhut, A.M. Brandt, D. Carmel, H.M. Silen, I. Vass, Y. Allahverdiyeva, T.A. Salminen, E.M. Aro, Operon *flv4-flv2* provides cyanobacterial photosystem II with flexibility of electron transfer, Plant Cell 24 (2012) 1952–1971.
[75] A. Badarau, S.J. Firbank, K.J. Waldron, et al., FutA2 is a ferric binding protein from *Synechocystis* PCC 6803, J. Biol. Chem. 283 (2008) 12520–12527.
[76] K.J. Waldron, S. Tottey, S. Yanagisawa, C. Dennison, N.J. Robinson, A periplasmic iron-binding protein contributes toward inward copper supply, J. Biol. Chem. 282 (2007) 3837–3846.
[77] A. Mehta, L. Lopez-Maury, F.J. Florencio, Proteomic pattern alterations of the cyanobacterium *Synechocystis* sp. PCC 6803 in response to cadmium, nickel and cobalt, J. Proteomics 102 (2014) 98–112.
[78] A.W. Foster, N.J. Robinson, Promiscuity and preferences of metallothioneins: the cell rules, BMC Biol. 9 (2011) 25–27;
R. Srivastava, T. Pisareva, B. Norling, Proteomic studies of the thylakoid membrane of *Synechocystis* sp. PCC 6803, Proteomics 5 (2005) 4905–4916.
[79] J.W. Lee, J.D. Helmann, Functional specialization within the Fur family of metallo-regulators, Biometals 20 (2007) 485–499.
[80] J.J.R. Frausto da Silva, R.J.P. Williams, The biological chemistry of the elements, Oxford University Press, Oxford, 2001.
[81] Y.O. Korshunova, D. Eide, W.G. Clark, M.L. Guerinot, H.B. Pakrasi, The IRT1 protein from *Arabidopsis thaliana* is a metal transporter with a broad substrate range, Plant Mol. Biol. 40 (1999) 37–44.
[82] M. Tikkanen, N.R. Mekala, E.M. Aro, Photosystem II photoinhibition-repair cycle protects Photosystem I from irreversible damage, Biochim. Biophys. Acta 1837 (2014) 210–215.